# COVID19 Lockdown has become a stairway of heaven for nature
# A case study of Delhi using geospatial technique

Sunaina Singh, Saumya Srivastava, Anish Ahmed, Chitralekha Das

**ABSTRACT:**
Urbanization is the result of anthropogenic activities that is responsible for the changes in nature. Environment is a very important factor for the life of human and other living beings. Rapid growth of urbanization, industrialization and transportation are disturbing the original nature of the specific area. Delhi is well known for one of the most pollutes cities on the global level. The study is focused on the adverse effect of human induced activities in the environment. $PM_{10}$ and NDBI analysis based maps are generated to understand the fluctuation of the values within a year. To analyze the intensity of human interference in the environment before and during COVID 19 lockdown and its impact, Delhi has been taken out for the study area. Optical data plays an important role to extract all the required data for environmental analysis. Landsat 8 data has been used of 28 April, 2019 & 30 April, 2020 for all parameter acquisitions and comparative analysis of $PM_{10}$, LST, NDVI and NDBI.
All these maps and graphs are generated for better qualitative and quantitative analysis. Relationship between all the above parameters helps a lot to understand the impact and relation of each parameter on the others. $PM_{10}$ data has been derived to analyze the fluctuation in data due to least human activities. NDBI is calculated to mark out the highly populated areas and its impact on the nature.
Anthropogenic activities are highly destructive for the nature and by analyzing its impact on the nature; government can make better policies and plans to reduce the human interference. Preserving the nature is very important to save human and other living beings lives. The proposed study can be helpful to analyze the negative impact of urbanization and the positive impact of lockdown on the nature.
**Keywords:** *COVID19, Urbanization, anthropogenic activities, Landsat 8, TIRS, DOS, PM10, LST, NDVI, NDBI, Multi linear regression.*
**Highlights:** *1. To understand the impact of anthropogenic activities in the environment.*
*2. To establish a relationship between Air Quality ($PM_{10}$) & other biosphere parameters during COVID 19 Pandemic.*

---

*Author: -Sunaina Singh, Citizen Resource Information Department (CRID), Haryana Space Application Centre, Hisar,125001), India, 8447822347, singhsunaina5221@gmail.com.*
*Co- Author: - Saumya Srivastava, Department of GIS Cell, DESTO, Vikas Bhawan, New Tehri, Garhwal, Uttrakhand, 249001 India, 7409036863, saumyasrivastvapp@gmail.com.*
*Anish Ahmed, Citizen Resource Information Department (CRID), Haryana Space Application Centre, Hisar,125001, India, 9540871718, anishahmed009@gmail.com.*
*Chitralekha Das, Citizen Resource Information Department (CRID), Haryana Space Application Centre, Hisar,125001, India, 8013399426, chitralekha9442@gmail.com.*

## INTRODUCTION

Urbanization is one of the key elements that are growing very rapidly in the present time globally. This process leads to drastic changes in a particular area from natural to artificial environments where urbanization is occurring. In the transition phase, various factors affect the environment badly and causes deterioration. COID-19 has created an economic crisis in India but for Mother Nature, it is not less than a boom. This lockdown has generated a very golden opportunity to analyze the quantitative and qualitative impact of anthropogenic activities on the environment and humans from local to a global level. COVID-19 outbreak was first to come to know in Wuhan city of China on 31 December 2019. The first case of novel corona virus was reported on 30 January 2020. The government announced the lockdown in the whole India, from 24 March 2020 to 3 May 2020. In present work, Delhi is taken as a case study to evaluate the impact of lockdown on the environment before lockdown and during the lockdown. In this study, Land surface temperature, Particulate Matter 10, and NDBI parameters are used to figure out the impact of these elements on urban society. Land surface temperature considers as one of the important factors in global change studies, estimating radiation budgets, heat balance studies, and as a controller for climate models. So, LST plays a major role in the study of its impact on human habitats and nature. Particulate matter (10 micrometers) has been considered as another major element in urban areas. $PM_{10}$ is responsible for increasing air pollution caused by building constructions especially. The population density factor is used to detect the nature of urbanization. Metro cities have high population density pressure compared to the city or town that results in high pollution and poor environment. So, the NDBI parameter is considered in this study to analyze the nature of population density over the study area. Fast-growing industrialization and urbanization, increment in population due to migration and natural births are one of the major causes of climatic change all over the world. Due to the high population in specific and limited areas, it results in a high population holding pressure on land that leads to increment in building density and pressure on building density leads to skyscrapers building constructions that again result out in the increasing rate of $PM_{10}$ on a large scale. With the development of satellite remote sensing technology since the 1960s, the ecological and environmental applications have undergone sustainable changes with the advancement of quantitative approaches. LST is highly influenced by the density of buildings that leads to an increase in the trapping of temperature that further helps to study the change detection in an urban environment[1]. Many studies show an existing strong proportional relationship between NDBI and LST[2]. Pertaining $PM_{10}$ concentration as an important factor, the study gets more impactful. Sustainable urban planning is comparatively a new practice that gives consideration to the environment and the quality of life of the inhabitants [3]. Present time, the most imperative problems in urban areas are the increasing rate of surface temperature, high population pressure and toxic pollution elements due to dramatic alteration of natural surfaces that are caused by the removal of natural vegetation and finally replaced by non-evaporating, non-transpiring surface (e.g. stone, metal, concrete, etc.), concretization, and abundance of pollutants in the surroundings.

With the development of technologies, remote sensing got more importance in comparison with the ground observation data, and also the abundance of availability, accessibility, and feasibility make it more useable. Thermal infrared (TIR) sensor is used to obtain quantitative information on surface temperature across the land surface. From NIR bands, the information of vegetative surface has gathered that fluctuate the distribution of LST, with the dense cover on the surface area the less penetration of solar radiation to the ground [4]. SWIR bands are used to give information about the built-up distribution area from where we can get the NDBI[5] as well as for Dark Object Subtraction Method for $PM_{10}$. The study is focused on the optical remote sensing technique approach. The main objective of the study is to analyze the impact of industrialization, transportation, building construction, and other anthropogenic activities on humans and nature. For better representation, Delhi has been taken for the study and 28 April 2019 and 30 April 2020 data sets have been used. Delhi is the capital of India, so continuous growth in urbanization and industrialization lead to enormous human concentration (mainly due to migration of people from small towns and villages in search of livelihood) that effectively increases pollution and population pressure. Considering the PM concentration detection, the final output of Landsat 8 visible data collaborates [6]with the ground truth data from Automated Weather Station of Delhi. Due to COVID-19 pandemic, India was completely shut down from March 2020 to April 2020. So, this lockdown has helped to heal the environment. The result shows a drastic positive change in the environment within a year due to a reduction in human activities.

## 2. DATA USED AND METHODOLOGY

- *In-situ* data for $PM_{10}$ from Automated weather station data
- Satellite imagery of LANDSAT 8

| Date | Sensor | Resolution | Source |
|---|---|---|---|
| 28 April, 2019 | Landsat OLI_TIRS | 30 m | USGS |
| 30 April, 2020 | Landsat OLI_TIRS | 30 m | USGS |
| 28 April, 2019 | $PM_{10}$ | NA | Ground Station |
| 30 April, 2020 | $PM_{10}$ | NA | Ground Station |

### 2.1. Derive Land Surface Temperature

#### 2.1.1. Top of Atmospheric Spectral Radiance Correction:

It is used to indicate the amount of emitted, reflected, transmitted, or received energy by a ground that has been captured by the sensor from a specific angle of view. The following formula is used to retrieve TOA spectral radiance ($L_\lambda$):

$$L_\lambda = M_L * Q_{cal} + A_L \text{.............. (1)}$$

Where,

$M_L$ = band-specific multiplicative rescaling factor

$Q_{cal}$ = band 10 image

$A_L$ = band-specific additive rescaling factor

### 2.1.2. Conversion of Radiance to At- Sensor Temperature:

After converting the DN values of band 10 into radiance, the next step is to convert the spectral radiance into brightness temperature. The metadata file is used to get temperature constants. The following algorithm is used to convert radiance to temperature brightness ($T_B$):

$$T_B = \frac{K2}{\ln\left[\left(\frac{K1}{L\lambda}\right)+1\right]} - 273.15 \text{ ............... (2)}$$

Where,

K1 and K2 are the band-specific thermal conversion constants from the metadata.

Here, -273.15 are used to get temperature brightness in degree centigrade (°C) unit instead of Kelvin

2.1.3. NDVI method for Emissivity Correction:

(a)Top of Atmospheric Reflectance Correction:

It is used to remove the effect of scattering and absorption from the atmosphere to obtain surface reflectance energy. Similar to the conversion to radiance, the 16-bit integer values in the L1 product can also be converted to TOA reflectance. The following equation is used to convert Level 1 DN values to TOA reflectance:

$$M_L * Q_{cal} + A_L / \sin(\theta) \text{ .................... (3)}$$

(b) NDVI calculation:

NDVI the calculation is important as it is a remarkable indicator of vegetation condition and its presence over a specific area. We have used Band 4 and Band 5 to get NDVI. NDVI is further used to retrieve the proportion vegetation condition (pvc) and emissivity (e) of the surface in estimate land surface temperature over the study area. NDVI is an important variable as it is more or less sensitive to estimate the soil moisture condition under the fully vegetated, partly vegetated and bare ground of the area.

$$NDVI = \frac{NIR\ (Band\ 5) - R\ (Band\ 4)}{NIR\ (Band\ 5) + R\ (Band\ 4)} \text{ ...........(4)}$$

(c) *pvc* calculation:

**TABLE: 1**
**CALCULATED NDVI AT DIFFERENT LOCATION OF DELHI (2019) & (2020)**

| AQI Ground Stations | NDVI 2019 | NDVI 2020 |
|---|---|---|
| Alipur, Delhi - DPCC | 0.18 | 0.20 |
| Anand Vihar, Delhi - DPCC | 0.08 | 0.25 |
| Ashok Vihar, Delhi - DPCC | 0.24 | 0.28 |
| Aya Nagar, Delhi - IMD | 0.22 | 0.23 |
| Bawana, Delhi - DPCC | 0.33 | 0.13 |
| CRRI Mathura Road, Delhi - IMD | 0.13 | 0.12 |
| Dr. Karni Singh Shooting Range, Delhi - DPCC | 0.21 | 0.23 |
| DTU, Delhi - CPCB | 0.25 | 0.19 |
| Dwarka-Sector 8, Delhi - DPCC | 0.12 | 0.19 |
| IGI Airport (T3), Delhi - IMD | 0.25 | 0.24 |
| ITO, Delhi - CPCB | 0.28 | 0.11 |
| Jahangirpuri, Delhi - DPCC | 0.18 | 0.23 |
| Jawaharlal Nehru Stadium, Delhi - DPCC | 0.41 | 0.31 |
| Major Dhyan Chand National Stadium, Delhi - DPCC | 0.11 | 0.32 |
| Mandir Marg, Delhi - DPCC | 0.15 | 0.24 |
| Mundka, Delhi - DPCC | 0.10 | 0.12 |
| Najafgarh, Delhi - DPCC | 0.17 | 0.18 |
| Narela, Delhi - DPCC | 0.13 | 0.11 |
| North Campus, DU, Delhi - IMD | 0.11 | 0.26 |
| Okhla Phase-2, Delhi - DPCC | 0.13 | 0.18 |
| Patparganj, Delhi - DPCC | 0.10 | 0.17 |
| Punjabi Bagh, Delhi - DPCC | 0.18 | 0.22 |
| Pusa, Delhi - DPCC | 0.06 | 0.29 |
| Pusa, Delhi - IMD | 0.18 | 0.18 |
| R K Puram, Delhi - DPCC | 0.16 | 0.27 |
| Rohini, Delhi - DPCC | 0.18 | 0.24 |
| Shadipur, Delhi - CPCB | 0.07 | 0.18 |
| Sirifort, Delhi - CPCB | 0.24 | 0.36 |
| Sonia Vihar, Delhi - DPCC | 0.11 | 0.25 |
| Sri Aurobindo Marg, Delhi - DPCC | 0.15 | 0.32 |
| Vivek Vihar, Delhi - DPCC | 0.12 | 0.19 |
| Wazirpur, Delhi - DPCC | 0.12 | 0.20 |

This is used to get a scaled value of NDVI ranging from 0 to 1. It reduces the reflectance error.

$$pvc = \left(\frac{NDVI - NDVIs}{NDVIv - NDVIs}\right)^2 \text{ ......................... (5)}$$

ISSN 2229-5518

Where,

$NDVI_S$ = NDVI reclassified for soil

$NDVI_\upsilon$ = NDVI reclassified for vegetation

(d) Land Surface Emissivity calculation:

$\varepsilon$- $pvc = 0.004 \times P\upsilon + 0.986$ ………………….. (6)

$$T_s = \frac{TB}{\{1+[(L\lambda * \frac{TB}{\rho})\ln(\varepsilon)]\}} \text{ ……………….. (7)}$$

Where, $T_s$ = LST in Celsius (°C)

TB = at- sensor brightness temperature (°C)

$L\lambda$ =wavelength of emitted radiance ($\lambda$ = 10.895)

$\varepsilon = \varepsilon - pvc$ (from equation 6)

$\rho = h\frac{c}{\sigma} = 1.438 \times 10^{-2}$ m K....…. (8)

**Table:2**
**Calculated LST at different location of Delhi (2019) & (2020).**

| AQI Stations | LST 2019 | LST 2020 |
|---|---|---|
| Alipur, Delhi - DPCC | 38 | 37 |
| Anand Vihar, Delhi - DPCC | 38 | 36 |
| Ashok Vihar, Delhi - DPCC | 36 | 36 |
| Aya Nagar, Delhi - IMD | 38 | 36 |
| Bawana, Delhi - DPCC | 37 | 39 |
| CRRI Mathura Road, Delhi - IMD | 36 | 36 |
| Dr. Karni Singh Shooting Range, Delhi - DPCC | 37 | 38 |
| DTU, Delhi - CPCB | 39 | 38 |
| Dwarka-Sector 8, Delhi - DPCC | 37 | 36 |
| IGI Airport (T3), Delhi - IMD | 38 | 37 |
| ITO, Delhi - CPCB | 36 | 35 |
| Jahangirpuri, Delhi - DPCC | 37 | 36 |
| Jawaharlal Nehru Stadium, Delhi - DPCC | 37 | 36 |
| Major Dhyan Chand National Stadium, Delhi - D | 35 | 34 |
| Mandir Marg, Delhi - DPCC | 37 | 38 |
| Mundka, Delhi - DPCC | 39 | 38 |
| Najafgarh, Delhi - DPCC | 39 | 39 |
| Narela, Delhi - DPCC | 39 | 38 |
| North Campus, DU, Delhi - IMD | 35 | 34 |
| Okhla Phase-2, Delhi - DPCC | 38 | 37 |
| Patparganj, Delhi - DPCC | 36 | 35 |
| Punjabi Bagh, Delhi - DPCC | 37 | 36 |
| Pusa, Delhi - DPCC | 39 | 37 |
| Pusa, Delhi - IMD | 36 | 37 |
| R K Puram, Delhi - DPCC | 36 | 35 |
| Rohini, Delhi - DPCC | 38 | 37 |
| Shadipur, Delhi - CPCB | 38 | 37 |
| Sirifort, Delhi - CPCB | 34 | 34 |
| Sonia Vihar, Delhi - DPCC | 38 | 36 |
| Sri Aurobindo Marg, Delhi - DPCC | 35 | 34 |
| Vivek Vihar, Delhi - DPCC | 37 | 37 |
| Wazirpur, Delhi - DPCC | 37 | 36 |

## 2.2. Derive $PM_{10}$ through geospatial technique:

### 2.2.1. Path Radiance (Using Dark object subtraction Method):

It is one of the easiest ways of atmospheric correction to reduce or correct atmospheric effects. It is used to examine air pollution in the atmosphere that is derived through an aerosol optical parameter [7]. It is assumed lowest digital number (DN) pixel value in each band should be zero and by this way, its radiometric DN value represents the addictive effect of the atmosphere. The basic assumption is that within the image some pixels are in complete shadow and their radiances received at the satellite are due to atmospheric scattering (path radiance). The objective of that improved dark-object method is to select spectral-band haze values that are correlated to each other, rather than by using the histograms of each spectral band independently, which can cause haze-selection problems when topographic shadow conditions are minimal[8]. It shows the relationship between the spectral aerosol optical thickness and the spectral path radiance. It adds to the surface radiance of the dark object and gives the radiance of the target to the sensor. The formula is given below (Camfer," Remote Sensing and Image Analysis", University at Berkeley):

$$L_P = L_W - L \text{ ……………………………… (9)}$$

Where,

LP = Path Radiance

LW= Radiance of band

L= Minimum file pixel value of the band

### 2.2.2. Atmospheric Correction:

It is worth pointing out that Landsat 8 images are provided with band-specific rescaling factors that allow for the direct conversion from DN to TOA reflectance. However, the effects of the atmosphere (i.e. a disturbance on the reflectance that varies with the wavelength) should be considered to measure the reflectance at the ground. As described by [8], the land surface reflectance (ϱ) is:

$\rho = \pi*(L\lambda - Lp)*d^2$ ………………………… (10)

$Tv*\{(ESUN\lambda*cos\theta*TZ)$

Where:

LP = path radiance (from equation 9)

TZ = atmospheric transmittance in the illumination direction

ESUNλ = mean solar exo-atmospheric irradiances

d = earth_sun distance (provided with Landsat 8 metadata)

2.2.3. Atmospheric Reflectance

It is used to reduce the atmospheric effects on the reflectance of the image. Atmospheric reflectance is calculated as: AR = TOA – Surface Reflectance……………………………… (11)

2.2.4. The final equation for PM10

derivation:



Particulate matter (PM10) pollution consists of very small liquid and solid particles floating in the air. PM10 particles are less than 10 microns in diameter.PM10 is a major component of air pollution that threatens both our health and our environment.

Particulate matter (PM), also known as particle pollution, is a complex mixture of extremely small particles and liquid droplets that get into the air. Once inhaled, these particles can affect the heart and lungs and cause serious health effects.

Here in this Study PM10 is estimated by Multiple Regression Analysis, the result was extended to a three and four-band algorithm as

A = e + e R1 + e R2 + e R3+ e R4………………………………(12)

Where

A = Particle concentration (PM10)

Ratm= Atmospheric reflectance, i = 0, 1 and 3 are the band number

ej=algorithm coefficients, j = 0, 1, 2, … are then empirically determined.

Form the equation; we found that PM10 is linearly related to the reflectance for band 1and band 2. This algorithm is generated based on the linear relationship between Ground data and atmospheric reflectance.

**Table: 3**
**Calculated PM10concentration from satellite image data and PM10 ground measurement at different location of Delhi (2019) & (2020).**

| AQI Stations | PM 10 Ground Station Based (µg/m3) 2019 | PM 10 estimated (µg/m3) 2019 | PM 10 Ground Station Based (µg/m3) 2020 | PM 10 estimated (µg/m3) 2020 |
|---|---|---|---|---|
| Alipur, Delhi - DPCC | 230 | 226 | 129 | 127 |
| Anand Vihar, Delhi - DPCC | 155 | 243 | 54 | 75 |
| Ashok Vihar, Delhi - DPCC | 246 | 166 | 50 | 54 |
| Aya Nagar, Delhi - IMD | 173 | 165 | 84 | 85 |
| Bawana, Delhi - DPCC | 157 | 164 | 133 | 136 |
| CRRI Mathura Road, Delhi - IMD | 219 | 215 | 109 | 112 |
| Dr. Karni Singh Shooting Range, Delhi - DPCC | 183 | 159 | 106 | 99 |
| DTU, Delhi - CPCB | 144 | 177 | 94 | 108 |
| Dwarka-Sector 8, Delhi - DPCC | 244 | 240 | 105 | 105 |
| IGI Airport (T3), Delhi - IMD | 131 | 164 | 87 | 89 |
| ITO, Delhi - CPCB | 130 | 155 | 94 | 96 |
| Jahangirpuri, Delhi - DPCC | 200 | 205 | 78 | 74 |
| Jawaharlal Nehru Stadium, Delhi - DPCC | 152 | 140 | 65 | 70 |
| Major Dhyan Chand National Stadium, Delhi - DPC | 135 | 211 | 56 | 57 |
| Mandir Marg, Delhi - DPCC | 250 | 243 | 58 | 60 |
| Mundka, Delhi - DPCC | 270 | 266 | 133 | 135 |
| Najafgarh, Delhi - DPCC | 226 | 232 | 137 | 127 |
| Narela, Delhi - DPCC | 260 | 257 | 189 | 188 |
| North Campus, DU, Delhi - IMD | 305 | 297 | 42 | 40 |
| Okhla Phase-2, Delhi - DPCC | 209 | 211 | 108 | 107 |
| Patparganj, Delhi - DPCC | 212 | 228 | 91 | 92 |
| Punjabi Bagh, Delhi - DPCC | 226 | 220 | 122 | 114 |
| Pusa, Delhi - DPCC | 256 | 254 | 63 | 64 |
| Pusa, Delhi - IMD | 205 | 202 | 63 | 66 |
| R K Puram, Delhi - DPCC | 226 | 229 | 51 | 68 |
| Rohini, Delhi - DPCC | 235 | 230 | 72 | 89 |
| Shadipur, Delhi - CPCB | 235 | 233 | 80 | 97 |
| Sirifort, Delhi - CPCB | 174 | 169 | 51 | 56 |
| Sonia Vihar, Delhi - DPCC | 259 | 261 | 44 | 56 |
| Sri Aurobindo Marg, Delhi - DPCC | 213 | 213 | 36 | 45 |
| Vivek Vihar, Delhi - DPCC | 255 | 259 | 60 | 79 |
| Wazirpur, Delhi - DPCC | 192 | 195 | 61 | 89 |

### 2.2.5. Normalized difference built-up index (NDBI):

This index is used to determine the urban areas or built-up areas. In remote sensing data, it is widely used where SWIR bands reflect high from urban area comparative to the NIR region. It is almost similar to NDVI, but working with different spectrum region.

Hence the formula is;

$$NDBI = \frac{Float\ (SWIR) - Float\ (NIR)}{Float\ (SWIR) + Float\ (NIR)}$$ ……… (13)

The value always ranges from -1 to +1, and here float is taken to give a continuous output of the data.

**Table: 2**

**Calculated NDB at different location of Delhi (2019) & (2020).**

| AQI Station | NDBI 2019 | NDBI 2020 |
|---|---|---|
| Alipur, Delhi - DPCC | -0.03 | -0.05 |
| Anand Vihar, Delhi - DPCC | 0.01 | -0.14 |
| Ashok Vihar, Delhi - DPCC | -0.12 | -0.17 |
| Aya Nagar, Delhi - IMD | -0.06 | -0.08 |
| Bawana, Delhi - DPCC | -0.13 | 0.01 |
| CRRI Mathura Road, Delhi - IMD | -0.04 | -0.03 |
| Dr. Karni Singh Shooting Range, Delhi - DPCC | -0.04 | 0.01 |
| DTU, Delhi - CPCB | -0.10 | -0.04 |
| Dwarka-Sector 8, Delhi - DPCC | -0.03 | -0.09 |
| IGI Airport (T3), Delhi - IMD | -0.12 | -0.13 |
| ITO, Delhi - CPCB | -0.16 | -0.02 |
| Jahangirpuri, Delhi - DPCC | -0.07 | -0.12 |
| Jawaharlal Nehru Stadium, Delhi - DPCC | -0.21 | -0.17 |
| Major Dhyan Chand National Stadium, Delhi - DPC | -0.06 | -0.17 |
| Mandir Marg, Delhi - DPCC | 0.00 | -0.09 |
| Mundka, Delhi - DPCC | 0.00 | 0.01 |
| Najafgarh, Delhi - DPCC | -0.04 | -0.01 |
| Narela, Delhi - DPCC | -0.02 | 0.03 |
| North Campus, DU, Delhi - IMD | -0.05 | -0.18 |
| Okhla Phase-2, Delhi - DPCC | -0.03 | -0.08 |
| Patparganj, Delhi - DPCC | -0.03 | -0.10 |
| Punjabi Bagh, Delhi - DPCC | -0.04 | -0.06 |
| Pusa, Delhi - DPCC | -0.01 | -0.19 |
| Pusa, Delhi - IMD | -0.08 | -0.08 |
| R K Puram, Delhi - DPCC | -0.06 | -0.15 |
| Rohini, Delhi - DPCC | -0.01 | -0.06 |
| Shadipur, Delhi - CPCB | 0.00 | -0.07 |
| Sirifort, Delhi - CPCB | -0.14 | -0.22 |
| Sonia Vihar, Delhi - DPCC | 0.02 | -0.10 |
| Sri Aurobindo Marg, Delhi - DPCC | -0.05 | -0.18 |
| Vivek Vihar, Delhi - DPCC | -0.06 | -0.03 |
| Wazirpur, Delhi - DPCC | -0.05 | -0.12 |

# 3. RESULTS:

## 3.1. Comparative analysis between 2019 and 2020 LST:

As from the graph 1, it has been clear that the temperature of 2020 was comparatively slight lower than the temperature of 2019.

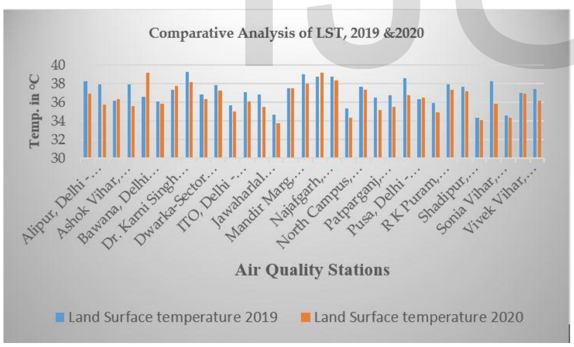


**Graph: 1. Comparative analysis between PM10 2019 and PM10 2020:**

During lockdown, it has been shown a drastic positive change in air quality. The value of $PM_{10}$ in 2020 was found very good comparative to 2019. From the graph 2, one can easily understand the huge and negative impact of anthropogenic activities on environment.


**Graph: 2. Comparative analysis between $PM_{10}$ 2019 and $PM_{10}$ 2020:**

Graph 3 represents the fluctuation of NDVI between 2019 and 2020 data. The graph clearly shows the upper range of NDVI of 2020 that means the quality of vegetation index was better than 2019. Due to least pollution during lockdown, the NDVI value has found increased.

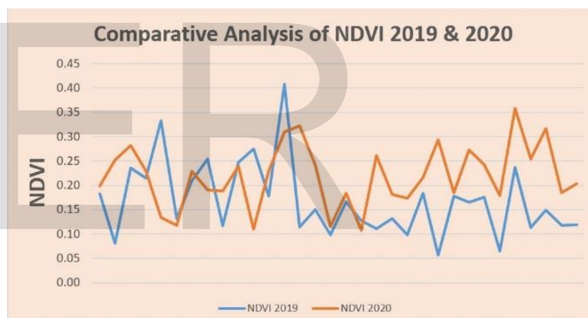


**Graph: 3. Comparative analysis between NDVI 2019 and NDVI 2020:**

NDBI plays a major role to understand the population and pollution of the specific area due to settlement area of human. Graph 3 shows a slight difference in the value of NDBI in 2019 and 2020. The fluctuation of 2020 NDBI is a little down to 2019 NDBI value.

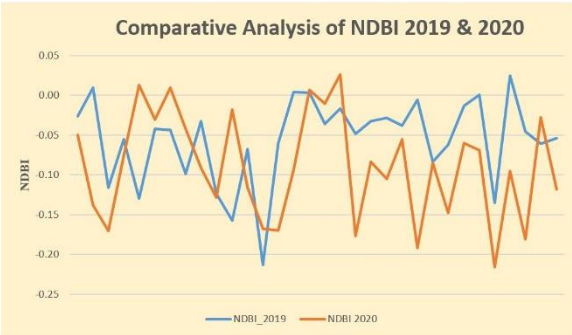


**Graph: 3. Comparative analysis between NDBI 2019 and NDBI 2020:**

**3.2. Relationship between satellite derived LST and satellite derived NDVI:**

Graph 4 and graph 5 represent the strong negative relationship between LST and NDVI of year 2019 and 2020 respectively. In the graph 4, regression is found 0.72 while in the graph 5, regression is 0.62 that proves an indirect relationship between temperature and the coverage of plant canopy.

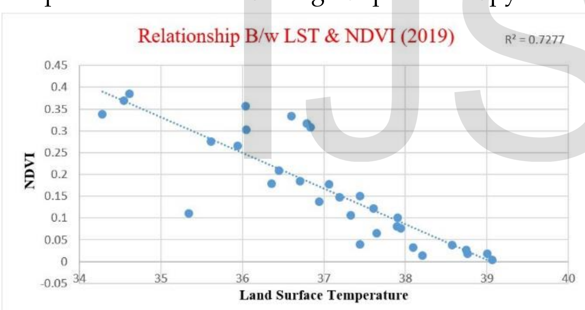


**Graph: 4. Relationship between satellite derived LST and satellite derived NDVI (2019):**

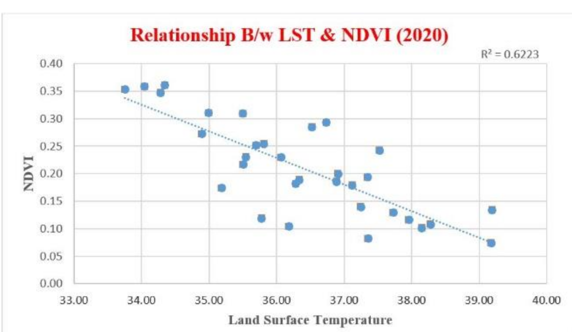


**Graph: 5. Relationship between satellite derived LST and satellite derived NDVI (2020):**

**3.3. Relationship between NDVI and NDBI:**

As we know that NDVI represents the canopy cover of flora kingdom and NDBI shows the buildup density so, it has a strong negative relationship with NDBI. Graph 6 has the scatter plot of NDVI and NDBI of year 2019 having the $R^2$ 0.75 while graph 7 has the scatter plot of NDVI and NDBI of year 2020 having the $R^2$ 0.73. From the graph 6 and graph 7, we can analyze that the lower the NDVI, the higher NDBI value is represented.

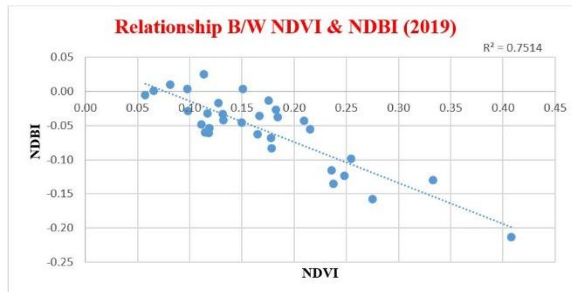


**Graph: 6. Relationship between NDVI and NDBI (2019).**

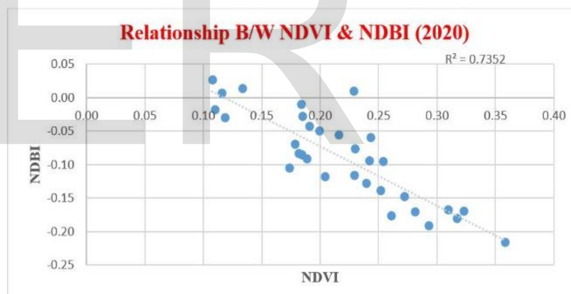


**Graph: 7. Relationship between NDVI and NDBI (2020).**

**3.4. Relationship between in- situ PM10 and satellite derived PM10:**

Graph 9 & graph 10 shows relation b/w satellite derived $PM_{10}$ and ground station based $PM_{10}$ of 2019 & of 2020 Graph 6 has the scatter plot of satellite derived $PM_{10}$ and ground station based $PM_{10}$ of year 2019 having the $R^2$ 0.87 while graph 7 has the scatter plot of satellite derived $PM_{10}$ and ground station based $PM_{10}$ of year 2020 having the $R^2$ 0.94.

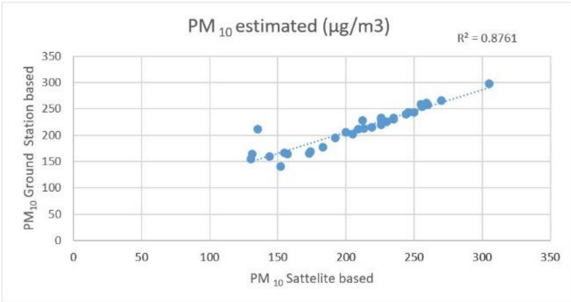


**Graph: 8.PM10 concentration from satellite image data and PM10 ground measurement at different location of Delhi (2019).**

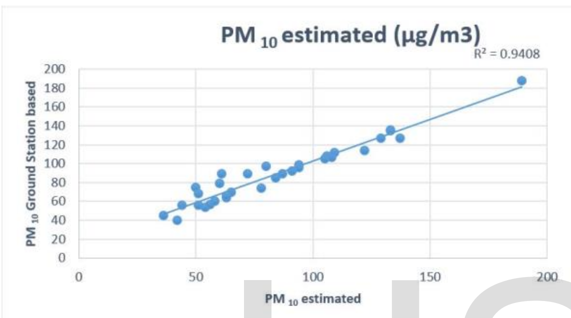


**Graph: 9.PM10 concentration from satellite image data and PM10 ground measurement at different location of Delhi (2020).**

### 3.5. Qualitative representation through maps:

In the following figures, the maps of LST, $PM_{10}$, NDVI and NDBI have been shown for comparative qualitative analysis. The maps are representing the difference between all the above parameter from year 2019 to year 2020.

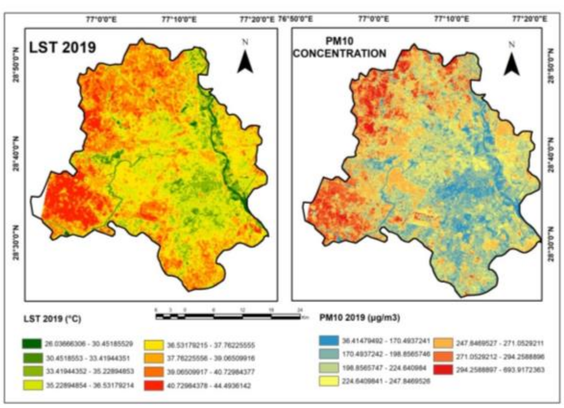


**Fig: 1. Relationship map of LST &PM10 of year 2019**

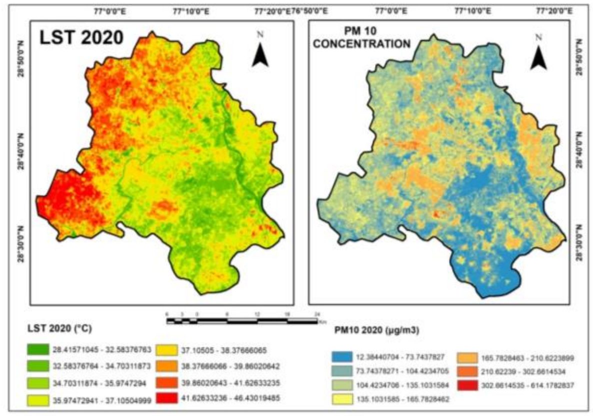


**Fig: 2. Relationship map of LST &PM10 of year 2020**

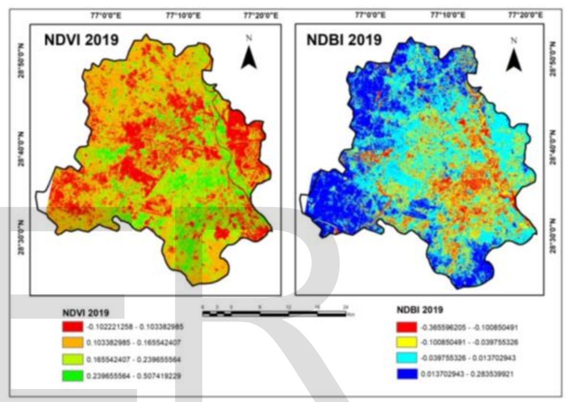


**Fig: 3. Relationship map of NDVI & NDBI of year 2019**

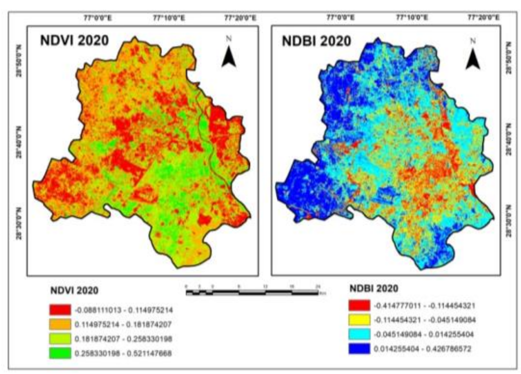


**Fig: 4. Relationship map of NDVI & NDBI of year 2020**

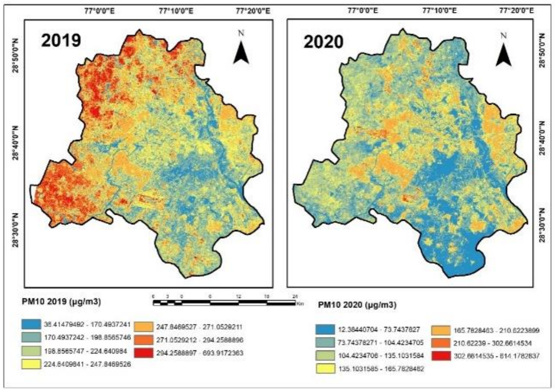


**Fig: 5. Comparative analysis map of $PM_{10}$ of year 2019 & 2020**

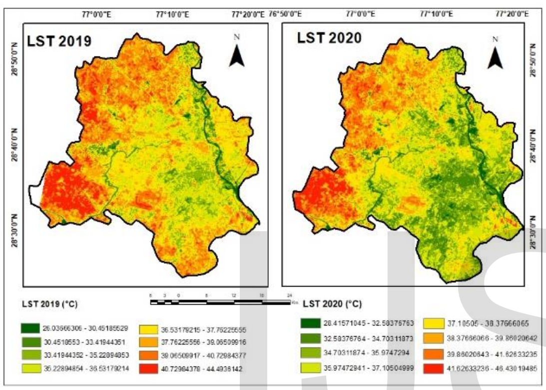


**Fig: 6. Comparative analysis map of LST of year 2019 & 2020**

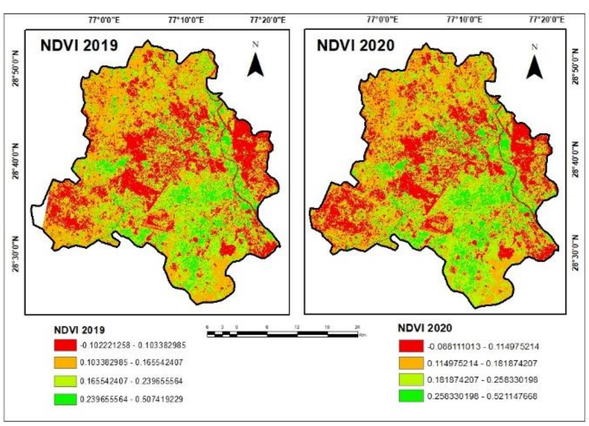


**Fig: 7. Comparative analysis map of NDVI of year 2019 & 2020**

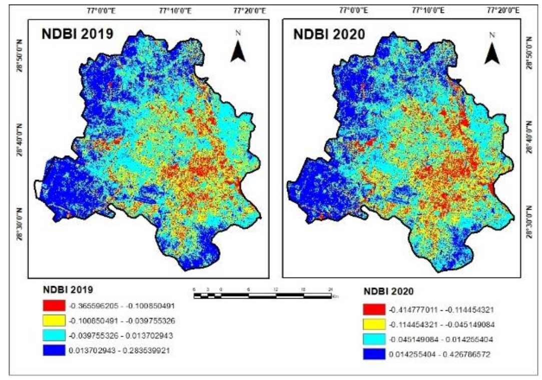


**Fig: 8. Comparative analysis map of NDBI of year 2019 & 2020**

## 5. DISCUSSION:

To achieve our objective, we have used Landsat 8 data for LST, $PM_{10}$ and NDBI derivation. Surface and Atmospheric correction was necessary to enhance the accuracy of results in $PM_{10}$. Dark Object Subtraction Method was used to avoid the haze and other atmospheric particles generated errors. Multiple Linear Regression methodology has been applied to achieve the quantitative value of $PM_{10}$for the study area. The map of $PM_{10}$ was generated to observe the difference of values in the both years. NDVI scatter plot was used to analyze the impact of lockdown on the vegetation while NDBI was derived to understand the role of buildings and over populated area in the environment. The study shows the positive impact of environment due to least human activities that might help government to make future planning and awareness among people accordingly.

## 6. CONCLUSION:

The Landsat 8 data has emerged as a very useful data to derive all the parameters that are essential to analyze the environmental impact. Optical data are used very limited due to its resolution, weather and cloud penetration limitation but its importance of Landsat 8 data for thermal analysis and easier techniques to obtain the objectives cannot be avoided. Delhi is one of the most polluted cities all over the world. There are lots of changes in the environment during the lockdown and before the lockdown due to least movement and industrial operations. The above study is very important to understand how humans have destroyed the beauty of nature. This analysis is focused on the adverse effect of environment in metropolitan cities. Migration and industrialization has affected the nature a lot. Man is nothing without nature. It is important to maintain the greenery for better health. Even though COVID 19 has affected economic condition of the world but we cannot ignore its drastic and positive impact on nature. The air quality has improved a lot in Delhi and is advisable for good health living. The vegetation index has also got better due to less pollution. The rate of built-up areas has also decreased that helped to produce low air polluted particles over the study area. The study analysis can be helpful for government to analyze the negative impact of anthropogenic activities and make the planning according to that while it can be useful for students and common people to understand the excessive interference of human in environment that disturbs the balance between man and nature.

## 7. References

[1] X.-L. Chen, H.-M. Zhao, P.-X. Li, and Z.-Y. Yin, “Remote sensing image-based analysis of the relationship between urban heat island and land use/cover changes,” *Remote Sens. Environ.*, vol. 104, no. 2, pp. 133–146, Sep. 2006, doi: 10.1016/j.rse.2005.11.016.

[2] P. Macarof and F. Statescu, “Comparasion of NDBI and NDVI as Indicators of Surface Urban Heat Island Effect in Landsat 8 Imagery: A Case Study of Iasi,” *Present Environ. Sustain. Dev.*, vol. 11, no. 2, pp. 141–150, Oct. 2017, doi: 10.1515/pesd-2017-0032.

[3] T. Yigitcanlar and Md. Kamruzzaman, “Planning, Development and Management of Sustainable Cities: A Commentary from the Guest Editors,” *Sustainability*, vol. 7, no. 11, pp. 14677–14688, Nov. 2015, doi: 10.3390/su71114677.

[4] J. Mallick, Y. Kant, and B. D. Bharath, “Estimation of land surface temperature over Delhi using Landsat-7 ETM+,” p. 10.

[5] S. S. Bhatti and N. K. Tripathi, “Built-up area extraction using Landsat 8 OLI imagery,” *GIScience Remote Sens.*, vol. 51, no. 4, pp. 445–467, Jul. 2014, doi: 10.1080/15481603.2014.939539.

[6] C. I. Alvarez-Mendoza, A. C. Teodoro, N. Torres, and V. Vivanco, “Assessment of Remote Sensing Data to Model PM10 Estimation in Cities with a Low Number of Air Quality Stations: A Case of Study in Quito, Ecuador,” *Environments*, vol. 6, no. 7, p. 85, Jul. 2019, doi: 10.3390/environments6070085.

[7] D. G. Hadjimitsis and C. Clayton, “Determination of aerosol optical thickness through the derivation of an atmospheric correction for short-wavelength Landsat TM and ASTER image data: an application to areas located in the vicinity of airports at UK and Cyprus,” *Appl. Geomat.*, vol. 1, no. 1–2, pp. 31–40, Jun. 2009, doi: 10.1007/s12518-009-0004-2.

[8] P. S. Chavez, “Image-Based Atmospheric Corrections - Revisited and Improved,” p. 12, 1996.

[9] Camfer,”Remote Sensing and Image Analysis”, University at Berkeley.